Electronic Supplementary Information

Crosslinking-Induced Anion Transport Control for Enhancing Linearity in Organic Synaptic Devices

Hyoik Jang,‡[a] Geun Yeol Bae,‡[b] Seung Hyun Kim,[c] Junho Sung,[a] and Eunho Lee[a]*

[a]Department of Chemical and Biomolecular Engineering, Seoul National University of Science and Technology, Seoul 01811, Republic of Korea
[b]Department of Material Design Engineering, Kumoh National Institute of Technology, Gumi 39177, Republic of Korea
[c]Department of Chemical Engineering, Pohang University of Science and Technology, Pohang 37673, Republic of Korea

‡These authors equally contributed to this work.

*** E-mail**: ehl@seoultech.ac.kr

Experimental Section

Materials and Synthesis. Trimethyltin chloride and diethylmethyl (2-methoxyethyl) ammonium bis(trifluoromethylsulfonyl) imide were purchased from Sigma-Aldrich. Thiophene was purchased from Tokyo Chemical Industry (TCI). 3,6-bis(5-bromothiophenyl)-2,5-bis(2-octyldodecyl) pyrrolopyrrole-1,4-dione was purchased from SunaTech. The 3-NIPS crosslinker ((oxybis(ethane-2,1-diyl)) bis(oxy)) (ethane-2,1-diyl) bis(4-azido2,3,5,6-tetra fluorobenzoate), was synthesized using the Steglich esterification method.[1,2] To synthesize 2, 5-bis(trimethylstannyl)thiophene. Thiophene (0.370 g) and tetramethyl ethylenediamine (1.071 g) were dissolved in 20 mL hexane, followed by the addition of 5.8 mL of n-butyllithium. The mixture was treated at 70 ℃ for 45 minutes and then cooled to 0 ℃. 9.3 mL of trimethyltin chloride was dropped to the solution in droplets. The solution was then stirred. The resulting solution was extracted with hexane. After washing with deionized water, it was dried over magnesium sulfate and vacuumed in a 10^{-2} torr vacuum oven for 24 hours to remove residual moisture and volatiles. Methanol was used for the recrystallization. PDPP3T was prepared by stille polycondensation using 0.180 g of 2, 5-bis(trimethyl stannyl)thiophene and 0.446 g of 3, 6-bis(5-bromothiophenyl)-2, 5-bis(2-octyldodecyl) pyrrolopyrrole-1, 4-diene dissolved in 15 mL of degassed toluene. A solution containing tri (*o*-tolyl)phosphine (0.12 eq) and $Pd_2(dba)_3$ (0.03 eq) was stirred for 12 h. Finally, the product was partitioned using methanol, hexane, and chloroform to obtain the chloroform fraction.

Device fabrications. The devices were fabricated on a p-type Si wafer with 285 nm of thermally grown SiO_2. The wafers, cut to a size of 1.5 cm x 1.5 cm, were cleaned by ultrasonication in ethanol for 20 minutes and dried by nitrogen blowing. To change the surface characteristics, the wafers were exposed to UV/ozone at 250 ℃ for 4 minutes. The solution for spin-coating was prepared by dissolving PDPP3T in chlorobenzene at a concentration of 7 μg/mL and stirring at 300 rpm for 20 minutes at 120 ℃. For PDPP3T/NIPS devices, 1 mg of 3-NIPS was added. The solution was spin-coated onto a SiO_2 substrate at 1500 rpm for 60 s and then exposed to UV light for 5 s for crosslinking. The devices were covered with shadow masks to deposit the electrodes. The channel length is 100 μm and width is 800 μm, and the gate electrode is 500 μm away from the channel. The source, drain, and gate electrodes were deposited with gold to a thickness of 40 nm using a thermal evaporator under 10^{-4} Pa. Finally, 30 μL of DEME-TFSI was dropped using a micropipette to cover the source, drain, and gate electrodes.

Measurement and analysis. The electrical properties of the devices were measured in a dark room in the air using a 4200A-SCS (Keithley Instruments) and B2902B (Keysight Technologies) semiconductor analyzer. GIWAXS measurements were performed at the 9A Ultra Small Angle X-ray Scattering Beamline of the PLS-II beamline at the Pohang Accelerator Research Center. X-ray photoelectron spectroscopy (XPS) was performed using a VersaProbe lll (ULVAC-PHI) microprobe.

Simulation of neural networks. The CNN simulation was performed in deep neural networks (DNN)+ NeuroSim. The VGG-8 structure for calculating the group classification accuracy consisted of six convolution and pooling layers and two fully connected layers. The CIFAR-10 image set was used for recognition training with 50000 images and classification training with 10000 images for 250 trials. To measure the device, the read voltage, pulse voltage, pulse width, *NL*, minimum and maximum conductances, and number of conductance states were used as parameters. ANN simulations were performed using NeuroSim ver. 3.0. The multilayer perceptron consists of 400 input neurons, 100 hidden neurons, and 10 output neurons, representing 0–9. Based on 60000 MNIST digits, 20000 training images were recognized, and the recognition accuracy was 10000 test images for 125 trials. The following parameters were used for the device measurement: read voltage, pulse voltage, pulse width, *NL*, minimum and maximum conductance, number of conductance states, and device variation.

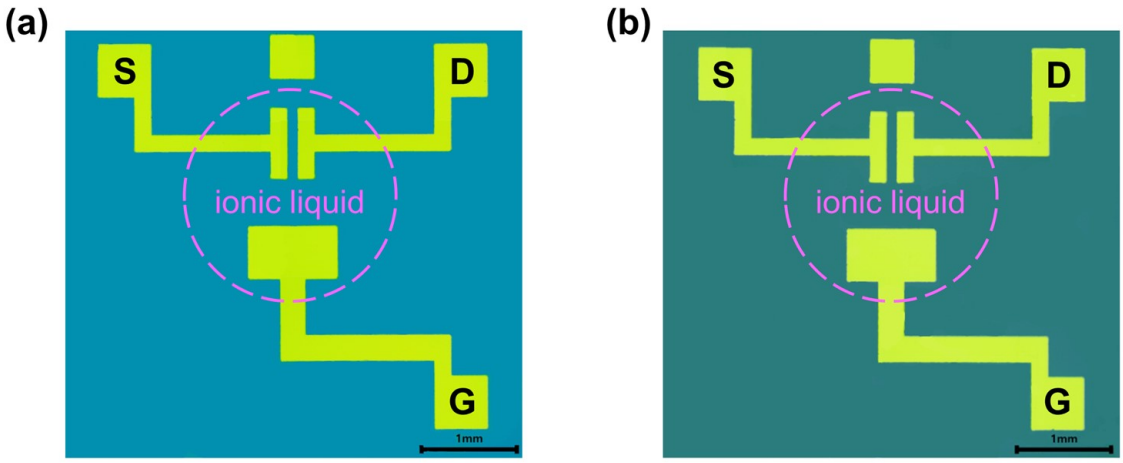

Fig. S1 Optical microscope images of (a) PDPP3T and (b) crosslinked PDPP3T/NIPS-based artificial synapses. The light purple circle with dashed lines represents the area occupied by DEME-TFSI ionic liquid.

Fig. S2 Molecular structures of DEME cation (left) and TFSI anion (right) that make up ionic liquid.

Fig. S3 Structural change in PDPP3T/NIPS blend upon UV crosslinking at a wavelength of 254 nm. The N_3 resonance of NIPS is changed by UV.

Table S1. Surface energy components of the polar and non-polar regions of the test liquids used for contact angle measurement.[3]

	$\gamma_l\,(mJ/m^2)$	$\gamma_l^p\,(mJ/m^2)$	$\gamma_l^n\,(mJ/m^2)$
Deionized water	72.8	51.0	21.8
Diiodomethane	50.8	0.0	50.8

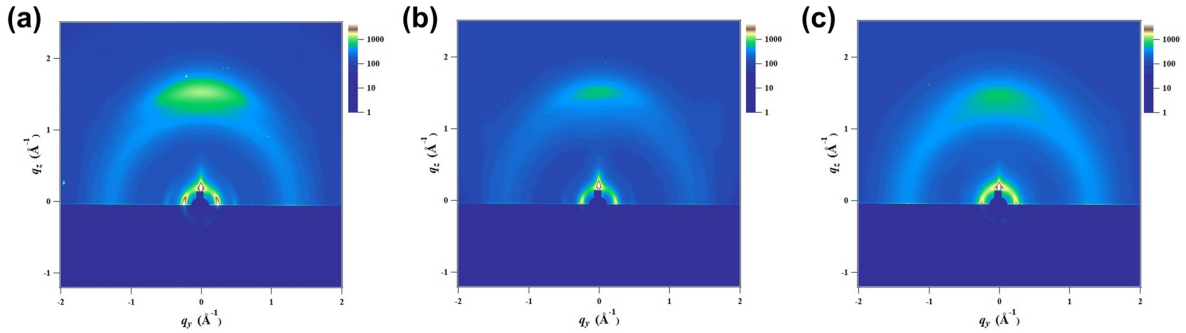

Fig. S4 GIWAXS mapping images of (a) PDPP3T, (b) blended PDPP3T/NIPS, and (c) crosslinked PDPP3T/NIPS.

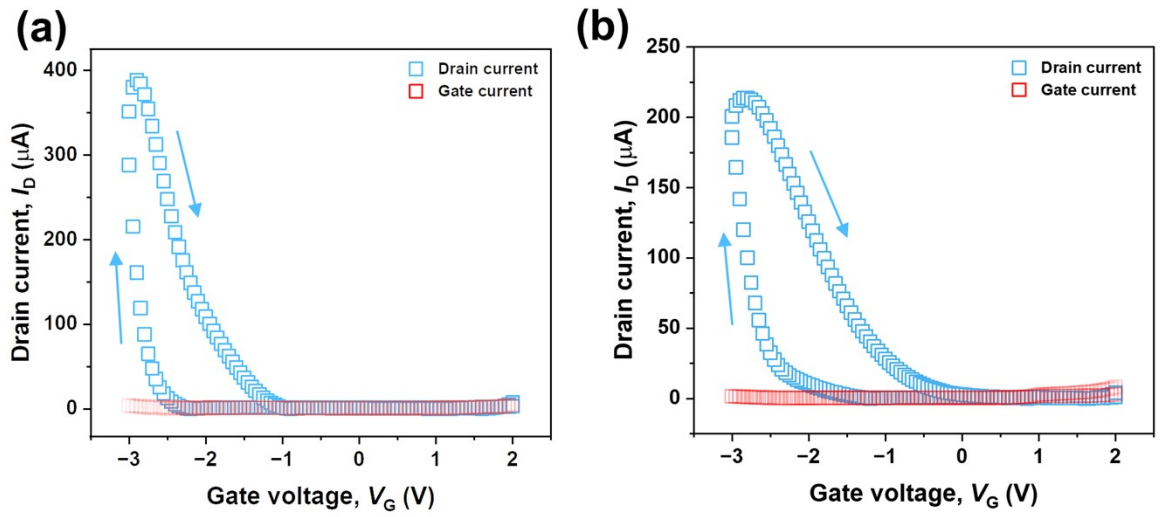

Fig. S5 Transfer curve of (a) PDPP3T and (b) PDPP3T/NIPS as shown by gate voltage double sweep from 2 V to -3 V at V_{DS} = -1 V.

Fig. S6 Short-term plasticity behavior for the 80 ms single pulse with different amplitudes in (a) PDPP3T and (b) PDPP3T/NIPS based devices at V_{DS} = -1 V. Inset: decay tendencies magnified view.

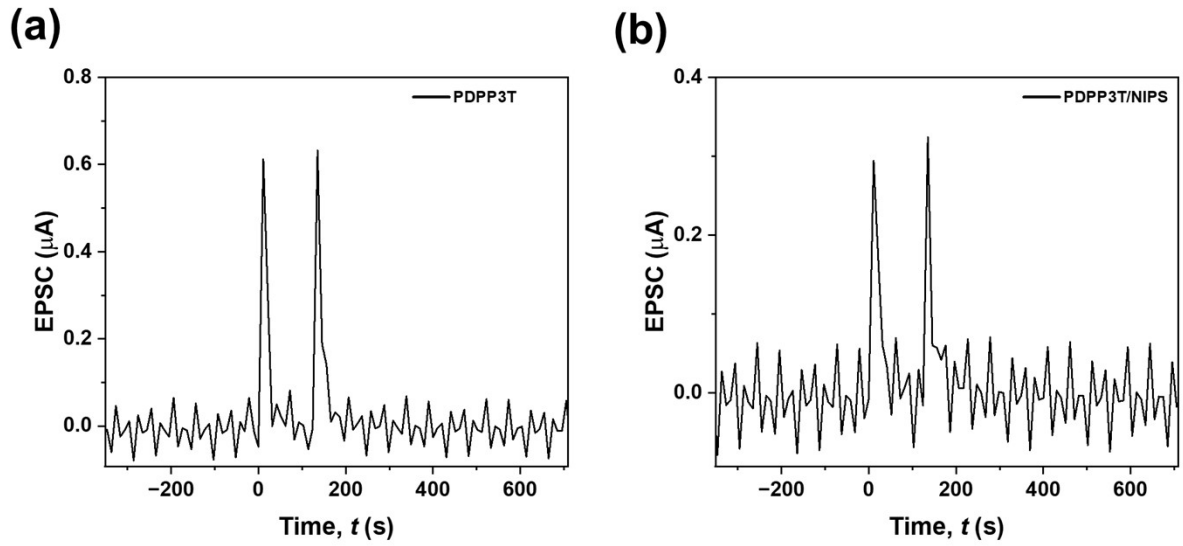

Fig. S7 Short-term plasticity of (a) PDPP3T and (b) PDPP3T/NIPS based synaptic devices upon application of low drain voltage (V_{DS} = -0.1 mV) and short electrical pulses (-2V, 20ms).

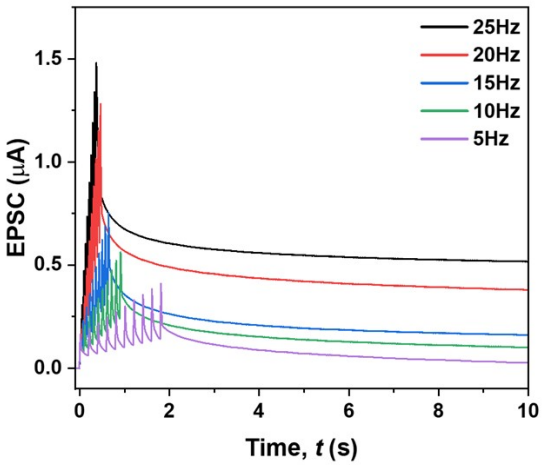

Fig. S8 EPSC behavior of PDPP3T/NIPS device by applying pulses (20 ms width, V_{pre} = - 2 V, V_{DS} = - 1 V) with different frequencies.

Fig. S9 Fitting curve to quantify the *NL* and the change in conductance as 50 negative (-2 V) and positive (+2 V) pulses are applied to the (a) PDPP3T and (b) PDPP3T/NIPS based device at V_{DS} = -0.7 V.

Fig. S10 Repetitive PSC changes over 50 cycles of operation on (a) PDPP3T and (b) PDPP3T/NIPS based devices. Each cycle consisted of 50 negative and positive pulses with width and interval of 80 ms at V_{DS} = -0.7 V

Fig. S11 Mean (red & blue dot) and standard deviation (bar) of PSCs recorded over 50 consecutive cycles in (a) PDPP3T and (b) PDPP3T/NIPS based devices.

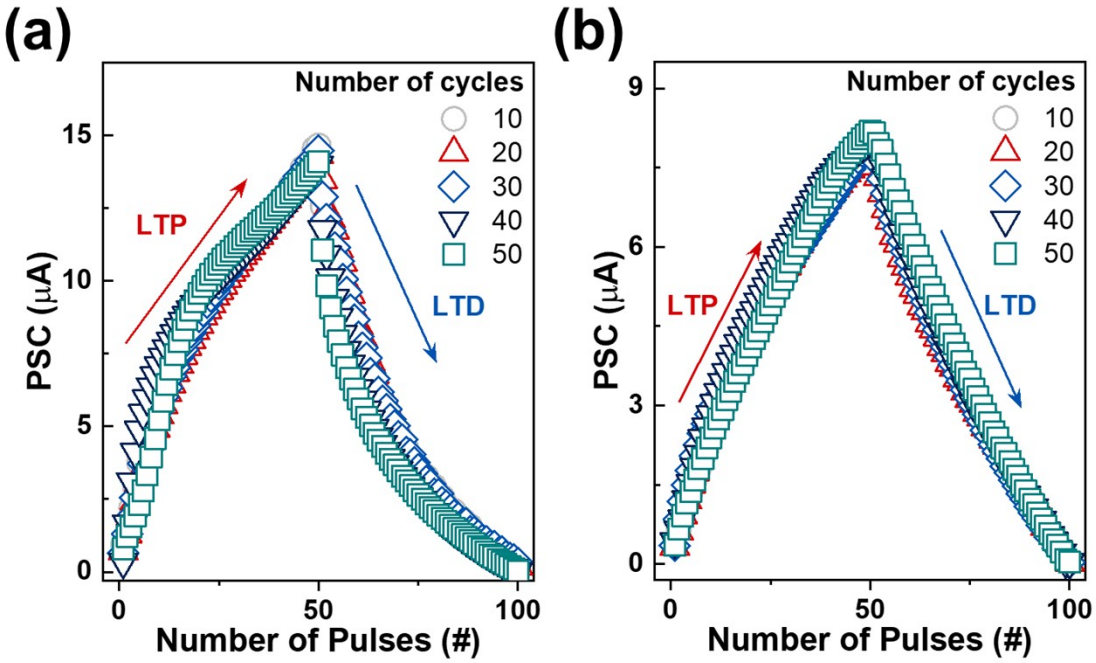

Fig. S12 PSC change in cycles of 50 consecutive negative and positive pulses selected in (a) PDPP3T and (b) PDPP3T/NIPS based devices

Fig. S13 Mean(red & blue dot) and standard deviation (bar) of PSC over 50 programming and erasing pulses on 10 devices of (a) PDPP3T and (b) PDPP3T/NIPS based devices, respectively.

Table S2. Benchmark table of reported various synaptic devices.

Semiconductor	Dielectric	Structure	Channel Width (Area) and Length	Hysteresis (Sweep range)	Switching speed (Operating pulse width)	Energy per spike	Potentiation and depression pulse condition	NL_{LTP} NL_{LTD}	Endurance (Pulse number)	MNIST accuracy (Integrated devices)	Ref.
MoS_2	h-BN	2T Floating gate	10 μm 3 μm	≈ 4 V (0 V ~ 12 V)	40 ns (100 ms)	18 fJ	10 V -10 V	0.18 0.29	55 cycles (5500)	97.7 % (1)	**4**
$SrTiO_3$ MgO	-	2T memristor	-	≈ 2 V (0 V ~ 4 V)	2 μs (-)	1.44 pJ	2 V ~ 7 V -2 V ~ -7 V	0.56 0.39	5 cycles (500)	97.5 % (1)	**5**
ZnO	K:TFSI	3T EGT	1600 μm 200 μm	2.673 V (-6 V ~ 6 V)	5 ms (20 ms)	~11 nJ	3.5 V -1.5 V	2.27 2.85	5000 cycles (3.2×10^5)	88.0 % (9)	**6**
Si	SiO2	3T Floating gate	5 μm 20 μm	≈ 4 V (-6 V ~ 8 V)	30 μs (500 μs)	50 fJ	5 V -3.3 V	0.96 0.89	2×10^5 cycles (2×10^6)	93.2 % (9)	**7**
P3HT	EMIM:TFSI PVDF-HFP	3T ion-gel vertical transistor	50×50 μm^2 55 nm	≈ 5 V (4 V ~ -4 V)	300 ns (50 ms)	0.17 nJ	-3 V 2 V	0.6 2.3	100 cycles (10^4)	92.5 % (1)	**8**
DPP-CNTVT:SVS	DEME:TFSI	3T EGT	600 μm 100 μm	≈ 2 V (2 V ~ -4 V)	20 ms (110 ms)	-	-4 V 4 V	0.14 5.91	4 cycles (400)	93.3 % (1)	**9**
PDVT-10 Ag NWs	PVDF-TrFE	3T FeFET	-	≈ 20 V (40 V ~ -40 V)	10 ms (10 ms)	1.2 nJ	-20 V 20 V	0.89 1.88	40 cycles (4000)	91.4 % (1)	**10**
ITO	Li:TFSI	3T EGT	400 μm 80 μm	≈ 3 V (-6 V ~ 10 V)	30 ms (60 ms)	7.29 pJ	1 V -0.2 V	1.5 4.1	-	76.0 % (1)	**11**
ZnO	$NaClO_4$ PEO	3T EGT	-	≈ 10 V (-10 V ~ 15 V)	250 ms (500 ms)	19.5 pJ	2 V ~ 9.56 V -2 V ~ -8.93 V	0.46 2.36	25 cycles (3200)	91.2 % (1)	**12**
MoS_2	-	2T memristor	-	≈ 1 V (0 V ~ 2 V)	20 ms (20 ms)	-	1 V -1 V	2.03 1.75	-	85.0 % (1)	**13**
PDPP3T NIPS	DEME:TFSI	3T OECT	800 μm 100 μm	1.06 V (2 V ~ -3 V)	20 ms (80 ms)	0.59 pJ	-2 V 2 V	0.54 0.83	50 cycles (5000)	90.1 % (10)	**This work**

Electronic Supplementary Information References

1. B. Neises, W. Steglich, *Angew. Chem. Int. Ed.,* 1978, 17, 522-524.
2. S. H. Kim, S. Chung, M. Kim, D. Yoo, E. Ok, S. Kim, K. C. Song, Y. J. Song, B. Kang, K. Cho, *Adv. Funct. Mater.*, 2023, **33**, 2212127.
3. N. Selvakumar, H. C. Barshiliad, K. S. Rajam, *J. Appl. Phys.,* **2010**, *108*, 013505.
4. J. Tang, C. He, J. Tang, K. Yue, Q. Zhang, Y. Liu, Q. Wang, S. Wang, N. Li, C. Shen, Y. Zhao, J. Liu, J. Yuan, Z. Wei, J. Li, K. Watanabe, T. Taniguchi, D. Shang, S. Wang, W. Yang, R. Yang, D. Shi, G. Zhang, *Adv. Mater.,* 2021, **31**, 2011083.
5. Z. Guo, G. Liu, Y. Sun, Y. Zhang, J. Zhao, P. Liu, H. Wang, Z. Zhou, Z. Zhao, X. Jia, J. Sun, Y. Shao, X. Han, Z. Zhang, X. Yan, *ACS Nano,* 2023, **17**, 21518-21530.
6. H. Lee, J. Cho, M. Jin, J. H. Lee, J. Kim, J. Lee, J. C. Shin, J. Yoo, E. Lee, Y. S. Kim, *ACS Nano,* 2024, **18**, 5383-5395.
7. S. Seo, B. Kim, D. Kim, S. Park, T. R. Kim, J. Park, H. Jeong, S.-O. Park, T. Park, H. Shin, M.-S. Kim, Y.-K. Choi, S. Choi, *Nat. Commun.,* 2022, **13**, 6431.
8. Y. Choi, S. Oh, C. Qian, J.-H. Park, J. H. Cho, *Nat. Commun.,* 2020, **11**, 4595.
9. D. Lee, L. Ayuningtias, J. Hwang, J. Sung, J. Kang, Y.-H. Kim, E. Lee, *ACS Mater. Lett.,* 2024, **6**, 2329-2338.
10. E. Li, X. Wu, Q. Chen, S. Wu, L. He, R. Yu, Y. Hu, H. Chen, T. Guo, *Nano Energy,* 2021, **85**, 106010.
11. J. Huang, J. Chen, R. Yu, Y. Zhou, Q. Yang, E. Li, Q. Chen, H. Chen, T. Guo, *Org. Electron.,* 2021, **89**, 106019.
12. Y. Park, M.-K. Kim, J.-S. Lee, *J. Mater. Chem. C,* 2021, **9**, 5396-5402.
13. J. Kim, C. Im, C. Lee, J. Hwang, H. Jang, J. H. Lee, M. Jin, H. Lee, J. Kim, J. Sung, Y. S. Kim, E. Lee, *Nanoscale Horiz.,* 2023, **8**, 1417-1427.